Optical activity probed with x-rays

2003 J. Phys.: Condens. Matter 15 S633

(http://iopscience.iop.org/0953-8984/15/5/316)

INSTITUTE OF PHYSICS PUBLISHING JOURNAL OF PHYSICS: CONDENSED MATTER

J. Phys.: Condens. Matter **15** (2003) S633–S645 PII: S0953-8984(03)54544-1

Optical activity probed with x-rays

José Goulon[1,4], Andrei Rogalev[1], Fabrice Wilhelm[1], Nicolas Jaouen[1], Chantal Goulon-Ginet[1,3] and Christian Brouder[2]

[1] European Synchrotron Radiation Facility, BP 220 F-38043 Grenoble, France
[2] Universités Paris-VI et VII, Laboratoire de Minéralogie-Cristallographie associé au CNRS, 4 place Jussieu, F-75252 Paris Cedex 05, France
[3] Université Joseph Fourier de Grenoble, Faculté de Pharmacie, 38706 La Tronche, France

E-mail: goulon@esrf.fr

Received 9 October 2002
Published 27 January 2003
Online at stacks.iop.org/JPhysCM/15/S633

Abstract

Optical activity (OA) was only recently discovered in the x-ray range. It is caused mainly by the electric dipole–electric quadrupole E1E2 interference terms which mix multipole moments of opposite parity and exist only in structures with *odd space parity*. OA related phenomena can be either *even* or *odd* with respect to time reversal: *natural* OA is concerned with time-reversal even effects whereas *non-reciprocal* OA refers to time-reversal odd contributions. Various types of x-ray dichroisms related to either natural or non-reciprocal OA have been detected and are reviewed in the present paper. Extra emphasis is put on two different non-reciprocal effects that were observed in selected magnetoelectric materials: (i) x-ray magnetochiral dichroism (XMχD) and (ii) the *non-reciprocal* x-ray magnetic linear dichroism. Edge-selective OA sum rules have recently been established which show that the effective operator of XMχD is the *orbital* anapole moment at the absorbing centre.

(Some figures in this article are in colour only in the electronic version)

1. Introduction

Natural optical activity (OA) at optical wavelengths was discovered early in the 19th century by Arago [1] and explained slightly later by Biot [2]. Unlike magneto-optical effects such as Faraday rotation or magnetic circular dichroism (MCD), which refer mainly to electric dipole (E1E1) transitions, OA is associated with transition probabilities which mix multipole moments of *opposite parity*, i.e. E1M1 or E1E2. The Curie principle teaches us immediately that this is only possible in systems with *odd space parity*. On the other hand, OA related effects can still be either even or odd with respect to *time-reversal* symmetry: time-reversal even OA properties such as optical rotation (OR) or circular dichroism (CD) are called by

[4] Author to whom any correspondence should be addressed.

tradition *natural*; time-reversal odd OA properties are much less common and are usually referred to as *non-reciprocal*. One should indeed be very careful not to confuse non-reciprocal OA properties with magneto-optical effects: both are time-reversal odd but these two classes of effects are of a different nature. Typically, non-reciprocal birefringence was predicted to be a rather small effect at optical wavelengths [3–5] and its existence was questioned for nearly 30 years until Krichevtsov *et al* [6] established that the corresponding effects could be perfectly well measured in the case of *magnetoelectric* (ME) solids. This pioneering experiment has stimulated our efforts to detect similar effects in the x-ray regime.

In the x-ray range, OA had long been ignored until x-ray natural circular dichroism (XNCD) was unambiguously detected at the ESRF in quite a few non-centrosymmetrical crystals [7–10]. There is, however, a major difference with respect to OA measurements carried out at optical wavelengths: for deep inner-shell spectroscopy, magnetic dipole (M1) transitions are forbidden by selection rules and the classical interference terms $\propto$ E1M1 contributing to the Rosenfeld–Condon rotatory strength are expected to vanish. Fortunately, in the x-ray regime there is quite a substantial contribution from the E1E2 cross terms which, in contrast, have a marginal contribution at optical wavelengths: it is the aim of the present paper to show that these E1E2 terms are responsible for both natural and non-reciprocal OA in the x-ray range. Extra emphasis will be put on the recent observation at the ESRF of two non-reciprocal dichroisms that have been detected in the low-temperature antiferromagnetic (AFM) phases of two ME single crystals:

- X-ray *magnetochiral* dichroism (XMχD) was detected below T_N in the AFM phase of Cr_2O_3 [11]. This dichroism is particularly fascinating because it is a property of the Stokes component S_0 which does not require any polarized x-ray beam but can be detected in powders as well as in single crystals.
- *Non-reciprocal* x-ray magnetic linear dichroism (nr-XMLD) has been observed in the AFM insulator phase of a chromium doped single crystal of $(V_{1-x}Cr_x)_2O_3$ [12]. In order to avoid any confusion, we would like to stress that this OA related magnetic linear dichroism is *time-reversal odd* as opposed to the magneto-optical XMLD effect discovered by Van der Laan *et al* [13] which is a time-reversal *even* effect proportional to the square of the magnetization.

In the next section, we will first recast the OA related dichroisms in the framework of the theory of refringent scattering, i.e. a theory elaborated long time ago by Buckingham and colleagues [14–16] for optical spectroscopy but which we have extended elsewhere [17] into the x-ray regime. This approach is convenient for identifying which are the various effects that can be measured experimentally in anisotropic media. We will indeed illustrate our predictions with experimental results including both natural and non-reciprocal dichroisms. In the last section, we would like to draw attention to the edge-selective OA sum rules derived recently by Carra and colleagues [18–20] which make it possible to identify the effective operators responsible for x-ray OA: in particular, we will show that XMχD spectra can give unique access to the projection of the *orbital* anapole moment $\boldsymbol{\Omega}$ along the direction of the wavevector $\boldsymbol{k}$. This reveals how closely OA and orbital magnetism are related.

2. Natural and non-reciprocal OA in the gyration tensor formalism

Let us consider transverse polarized light propagating along the direction $\boldsymbol{u}_\gamma$ and let us further assume that all x-ray modes propagating inside the crystal are nearly parallel to the incident wavevector $\boldsymbol{k}$. The latter assumption is particularly realistic with x-rays because the refractive

index $n = 1 - \delta$ is very close to unity ($\delta \leqslant 10^{-5}$). The complex forward scattering amplitude can then be expanded as:

$$a^*_{\alpha\beta} = \alpha^*_{\alpha\beta} + \zeta^*_{\alpha\beta\gamma}\boldsymbol{u}_\gamma + \omega^2[\tfrac{1}{4}C^*_{\alpha\gamma\gamma\beta} + \tfrac{1}{6}\eta^*_{\alpha\gamma\gamma\beta}][\boldsymbol{u}_\gamma]^2 + \cdots$$

where the first term on the right-hand side can be identified with the rank-2 electric dipole complex polarizability tensor ($\alpha^* \propto$ E1E1); the second term, which is most important for OA, is the rank-3 complex gyration tensor ($\zeta^* \propto$ E1E2 or E1M1); the next term involves at strictly the same level of approximation the *pure* electric quadrupole polarizability tensor ($C^* \propto$ E2E2) and the electric dipole–electric octupole interference term ($\eta^* \propto$ E1E3) which are both complex rank-4 tensors. It may be worth emphasizing that the electric dipole–electric octupole interference terms mix multipole moments of the same parity and thus do not contribute to OA. Regarding the parity mixing interference terms E1E2 $= A + \mathrm{i}A'$ and E1M1 $= B + \mathrm{i}B'$, the following identification is straightforward using the earlier work of Buckingham [14] or Barron [15]:

$$A_{\alpha\beta\gamma}(F) = +\frac{2}{\hbar}\sum_j \omega_{ij} F\,\mathrm{Re}\{\langle \mathrm{i}|E1_\alpha|j\rangle\langle j|E2_{\beta\gamma}|\mathrm{i}\rangle\}$$

$$A'_{\alpha\beta\gamma}(F) = -\frac{2}{\hbar}\sum_j \omega F\,\mathrm{Im}\{\langle \mathrm{i}|E1_\alpha|j\rangle\langle j|E2_{\beta\gamma}|\mathrm{i}\rangle\}$$

$$B_{\alpha\beta}(F) = +\frac{2}{\hbar}\sum_j \omega_{ij} F\,\mathrm{Re}\{\langle \mathrm{i}|E1_\alpha|j\rangle\langle j|M1_\beta|\mathrm{i}\rangle\}$$

$$B'_{\alpha\beta}(F) = -\frac{2}{\hbar}\sum_j \omega F\,\mathrm{Im}\{\langle \mathrm{i}|E1_\alpha|j\rangle\langle j|M1_\beta|\mathrm{i}\rangle\}$$

where the complex lineshape $F(\omega) = f(\omega) + \mathrm{i}g(\omega)$ combines both the dispersive (f) and the absorptive (g) Lorentzian lineshapes. It is convenient to separate next the imaginary and the real parts of the gyration tensor:

$$\mathrm{Im}\{\zeta^*_{\alpha\beta\gamma}\} = -\tfrac{1}{2}\omega\,\mathrm{Re}\{[\mathrm{E1E2}]_{\alpha\beta\gamma} - [\mathrm{E1E2}]_{\beta\alpha\gamma}\} + \mathrm{Im}\{\varepsilon_{\delta\gamma\alpha}[\mathrm{E1M1}]_{\beta\delta} - \varepsilon_{\delta\gamma\beta}[\mathrm{E1M1}]_{\alpha\delta}\}$$

$$\mathrm{Re}\{\zeta^*_{\alpha\beta\gamma}\} = +\tfrac{1}{2}\omega\,\mathrm{Im}\{[\mathrm{E1E2}]_{\alpha\beta\gamma} + [\mathrm{E1E2}]_{\beta\alpha\gamma}\} + \mathrm{Re}\{\varepsilon_{\delta\gamma\alpha}[\mathrm{E1M1}]_{\beta\delta} + \varepsilon_{\delta\gamma\beta}[\mathrm{E1M1}]_{\alpha\delta}\}.$$

As pointed out by Barron [15], the imaginary part of the complex gyration tensor is anti-Hermitian since: $\mathrm{Im}\{\zeta^*_{\alpha\beta\gamma}\} = -\mathrm{Im}\{\zeta^*_{\beta\alpha\gamma}\}$ and it is time-reversal *even*: this is the term responsible for *natural* OA. On the other hand, $\mathrm{Re}\{\zeta^*_{\alpha\beta\gamma}\}$ is Hermitian and time-reversal *odd*: this is the term responsible for non-reciprocal OA. Restricting ourselves to the absorptive part (g) of the gyration tensor, it can be shown that for every component of the Stokes polarization vector there is a specific dichroism related to OA:

(i) For the Stokes component $S_0 \Rightarrow$ non-reciprocal XMχD

$$\sigma^{I0}(H^+) - \sigma^{I0}(H^-) \propto \mathrm{Re}\{\zeta^*_{\beta\beta\gamma}(g) + \zeta^*_{\alpha\alpha\gamma}(g)\}.$$

(ii) For the Stokes component $S_1 \Rightarrow$ non-reciprocal XMLD

$$\sigma^{90^\circ}(H^\pm) - \sigma^{0^\circ}(H^\pm) \propto \mathrm{Re}\{\zeta^*_{\beta\beta\gamma}(g) - \zeta^*_{\alpha\alpha\gamma}(g)\}.$$

(iii) For the Stokes component $S_2 \Rightarrow$ non-reciprocal Jones cross XMLD

$$\sigma^{135^\circ}(H^\pm) - \sigma^{45^\circ}(H^\pm) \propto \mathrm{Re}\{\zeta^*_{\alpha\beta\gamma}(g)\}.$$

(iv) For the Stokes component $S_3 \Rightarrow$ XNCD

$$\sigma^L - \sigma^R \propto 2\,\mathrm{Im}\{\zeta^*_{\alpha\beta\gamma}(g)\}.$$

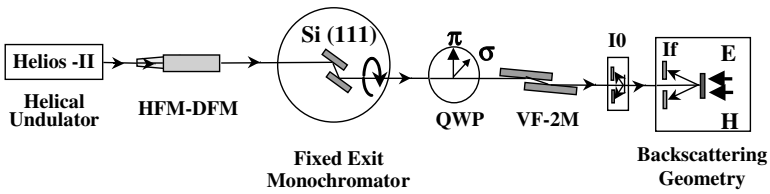

Figure 1. Conceptual block diagram of the ESRF beamline ID12. Abbreviations: HFM-DFM = horizontally focusing and deflecting mirrors; QWP = quarter-wave plate assembly; VF-2M = vertically focusing double mirror; I_0 = photodiode intensity monitor.

3. Instrumentation and experimental considerations

The experiments reported in this paper were all carried out at the ESRF beamline ID12A. Since the general performance of this beamline has already been detailed elsewhere [21, 22] we simply wish to emphasize here a few points which are particularly relevant for OA experiments. Three different helical undulators covering different energy ranges are available: the hybrid electromagnet/permanent magnet helical undulator (EMPHU) [23] is most appropriate for experiments at low photon energy ($E \leqslant 4$ keV) but makes it possible to flip very rapidly the circular polarization of the emitted photons from left to right; the undulators of the types Helios-II (HU-52) or Apple (HU-38) offer at a much longer timescale perfect control of the polarization with higher fluxes at higher energy. The concept of the beamline is illustrated schematically in figure 1: a first pair of SiC mirrors deflecting in the horizontal plane (HFM-DFM) and located upstream with respect to the fixed-exit double-crystal monochromator act essentially as a low-pass filter to reduce the heat load on the most critical component which is the monochromator itself; another pair of SiC mirrors now deflecting the beam in the vertical plane (VF-2M) is located behind the monochromator and is most conveniently used to get rid of the harmonics by as much as six orders of magnitude and to focus the beam vertically whenever it is needed.

One major problem for XNCD experiments is the transfer of circular polarization by the monochromator: it has long been known that the Stokes–Poincaré circular polarization rate P_3 vanishes rapidly when the Bragg angle approaches 45° but one has also to realize that reverting the helicity of the photons emitted by the undulator *does not revert ideally the helicity of the monochromatic beam at the sample*, especially when the undulator beam contains a significant amount of component P_2 which is severely altered by the monochromator. This problem has been considered in detail elsewhere [22, 24] and we wish to stress here that this can have dramatic consequences for both natural or non-reciprocal OA measurements in biaxial systems. As apparent from figure 1, a diamond quarter-wave plate (QWP) can be inserted after the monochromator: this device makes it possible to convert efficiently circularly polarized photons into (σ, π) linearly polarized x-ray photons with the advantage that one can switch rapidly from one linear polarization to the orthogonal one [25]. A linear polarimeter (not shown in figure 1) can eventually be inserted in front of the sample in order to measure accurately the polarization rate of the incident x-ray beam.

Nearly all OA experiments carried out at the ESRF concerned thick single crystals which were much too absorbing for measurements in the transmission mode. All spectra were then systematically recorded in the total fluorescence yield mode using photodiodes as detectors. The backscattering geometry of these detectors was found most attractive since it makes it possible:

(i) to set the optical axis of the crystal perfectly collinear with the wavevector $\boldsymbol{k}$ of the incident x-ray photons;
(ii) to rotate the crystal around the direction of the wavevector $\boldsymbol{k}$.

The latter option is crucial for OA experiments on non-uniaxial systems. Last, but not least, in the case of ME solids the sample can be inserted inside a cryomagnet so that a magnetic field $\boldsymbol{H}$ and an electric field $\boldsymbol{E}$ both parallel to the wavevector $\boldsymbol{k}$ can be applied simultaneously for ME annealing.

The following differential fluorescence excitation spectra (F) have been recorded for variable polarization states (j) of the incident x-ray beam I_0^j propagating along the z-axis:
$\Rightarrow$ x-ray natural circular dichroism

$$\mathrm{XNCD} = F(I_0^L) - F(I_0^R) \propto 2I_0 P_3 \,\mathrm{Im}\{\zeta^*_{xyz}\}\mu_T^{-1}$$

$\Rightarrow$ non reciprocal x-ray magnetochiral dichroism

$$\begin{aligned}\mathrm{XM}\chi\mathrm{D} &= [F(I_0^L, H\uparrow) + F(I_0^R, H\uparrow)] - [F(I_0^L, H\downarrow) + F(I_0^R, H\downarrow)] \\ &\propto 2I_0|P_3|\mathrm{Re}\{\zeta^*_{yyz} + \zeta^*_{xxz}\}\mu_T^{-1}\end{aligned}$$

$\Rightarrow$ non reciprocal x-ray magnetic linear dichroism

$$\mathrm{XMLD} = F(I_0^{90^\circ}, H\uparrow) - F(I_0^{0^\circ}, H\uparrow) \propto 2I_0 P_1 \,\mathrm{Re}\{\zeta^*_{yyz} - \zeta^*_{xxz}\}\mu_T^{-1}$$

where $\mu_T^{-1} = (\mu(E) + \mu(E_F))^{-1}$ is the usual homographic function responsible for isotropic fluorescence reabsorption [17].

4. Experimental evidence of natural OA of x-rays

One cannot expect to detect XNCD with all samples that are optically active in the visible. One should first bear in mind that the Cartesian E1E2 tensor is traceless and has no scalar part: this is indeed consistent with the *orthogonality* of the spherical harmonics Y_1^m and Y_2^m which are irreducible representations for the transition electric dipole and electric quadrupole in $SO(3)$. This has the important practical consequence that there is virtually no hope of detecting XNCD spectra in powdered samples: it is mandatory to use single crystals or oriented liquid crystals that have a strong rotational order. Similarly, not all crystals with odd space parity will exhibit natural OA in the x-ray range. Following Jerphagnon and Chemla [26], we have summarized in table 1 which ones of the 21 classes of non-centrosymmetric crystals are compatible with the detection of XNCD: only the crystal classes which admit a *pseudo-deviator* as rotational invariant in $SO(3)$ can exhibit XNCD associated with the ζ^* (E1E2) gyration tensor.

As a pedagogical example [9], we have reproduced in figure 2(a) the cobalt K-edge XANES (x-ray absorption near-edge structure) and XNCD spectra recorded with two enantiomeric single crystals of a chiral '*propeller-like*' organometallic complex $2[Co(en)_3Cl_3]\cdot NaCl\cdot 6H_2O$, in which the ligand field has the enantiomorphic D_3 point group symmetry. It immediately appears that the XNCD signal is not marginally small (0.8%) in the pre-edge region and, as expected, has opposite sign for the two enantiomers. Interestingly, we have also compared in figure 2(b) XNCD spectra recorded either with a single crystal or a pellet of a powdered sample of the same enantiomer. In the case of the powdered sample, there is only a very weak XNCD signal (amplitude 2.5×10^{-4}) which has *the opposite sign* with respect to the XNCD measured with the single crystal. There is indeed no way to transform a given enantiomer into its mirror image by some residual orientational order: it is therefore our interpretation that the weak signal observed with the powdered sample is of a different nature and is associated with a very small E1M1 scalar interference term. Indeed, *monoelectronic* M1 transitions

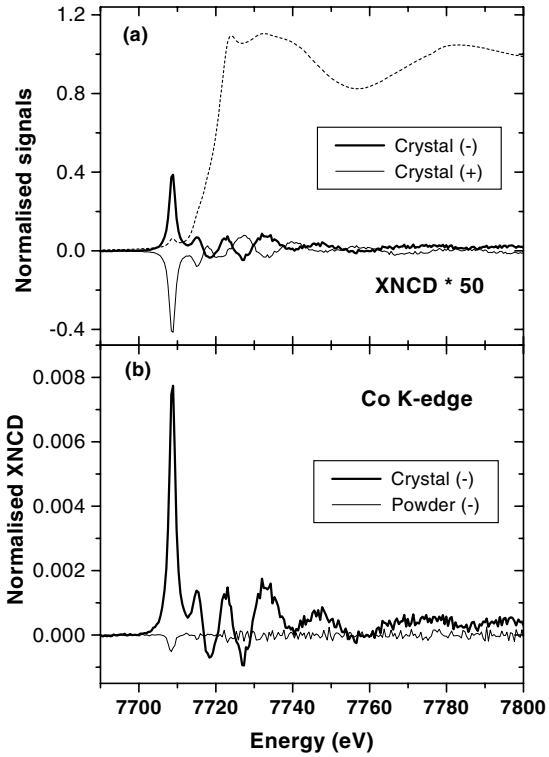

Figure 2. Co K-edge XNCD of the resolved enantiomers of the chiral complex: 2 $[Co(en)_3Cl_3]\cdot NaCl\cdot 6H_2O$. (a) XNCD spectra recorded with single crystals of the (+) and (−) enantiomers. A polarization averaged XANES spectrum was added for the sake of comparison. (b) XNCD spectra ot the (−) enantiomer as single crystal or as a powdered pellet. Note the very weak (but real) inverted signal of the powdered sample.

from a spherically symmetric 1s core level are strictly forbidden but the E1M1 transitions can still become allowed for a multielectron process such as a *two*-electron excitation involving for instance the transition of one core electron toward a fully symmetric A1 state and a simultaneous d → d transition.

We would also to point out the fact that quite a few *ab initio* simulations of XNCD spectra have now been successfully performed in the framework of the MSW theory of XNCD first developed by Natoli *et al* [27]. Typically, the experimental XANES and XNCD spectra recorded at the iodine L_I edge of a α-$LiIO_3$ single crystal are directly compared with MSW calculations performed by Goulon *et al* [7] using self-consistent potentials. Note that for this enantiomorphic crystal (space group: $P6_3$; point group C_6) the measured XNCD signal can be as large as 6% and is not peaking at the maximum of the strong white line but at the maximum of the nearest shape resonance. The large intensity of the XNCD signal of α-$LiIO_3$ has also been confirmed by Ankudinov and Rehr [28] who ran their relativistic FEFF8.10 code with much larger clusters of 100–140 atoms. For biaxial crystals of KTP, very promising simulations of the XNCD spectra were also obtained recently by Benayoun [29] using the elegant code FDMNES of Joly [30] which makes it possible to get rid of the critical *muffin-tin* approximation but unfortunately at the expense of very long computation times.

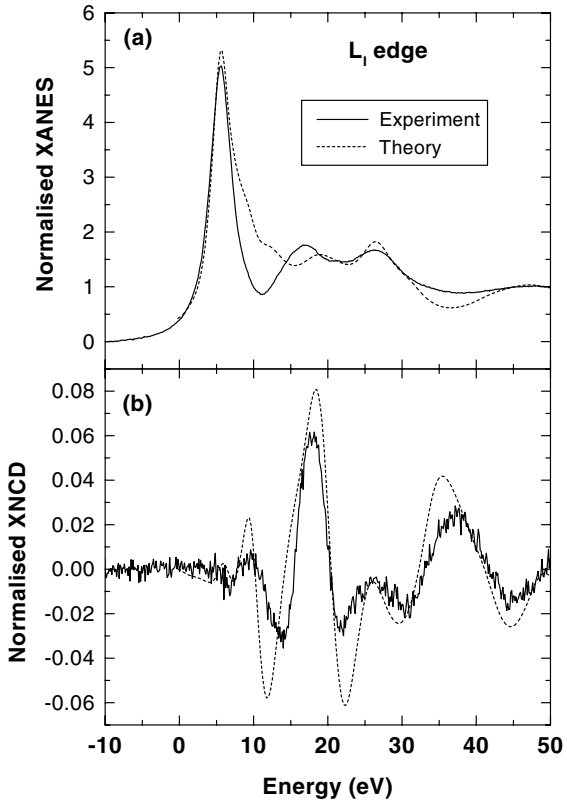

Figure 3. Comparison of the experimental and *ab initio* simulated iodine L_I edge XANES (a) and XNCD (b) spectra of an enantiomorphic α-$LiIO_3$ single crystal.

Table 1. Irreducible parts of OA in $SO(3)$.

Odd-parity crystal classes	Point groups	Pseudo-scalar Enantiomorphism	Polar vector Voigt/Fedorov	Pseudo-deviator XNCD
$\bar{4}3m$ $\bar{6}m2$ $\bar{6}$	T_d D_{3h} C_{3h}	−	−	−
432 23	O T	+	−	−
622 32 422	D_6 D_3 D_4	+	−	+
$6mm$ $3m$ $4mm$	C_{6v} C_{3v} C_{4v}	−	+	−
6 3 4	C_6 C_3 C_4	+	+	+
$\bar{4}2m$	D_{2d}	−	−	+
$\bar{4}$	S_4	−	−	+
$mm2$	C_{2v}	−	+	+
222	D_2	+	−	+
2	C_2	+	+	+
m	C_s	−	+	+
1	C_1	+	+	+

5. Experimental evidence of non-reciprocal OA of x-rays

At first glance, ME solids appear to be good candidates for detecting non-reciprocal OA effects because, as pointed out by Dzyaloshinskii [31], the ME tensor is known to be odd with respect

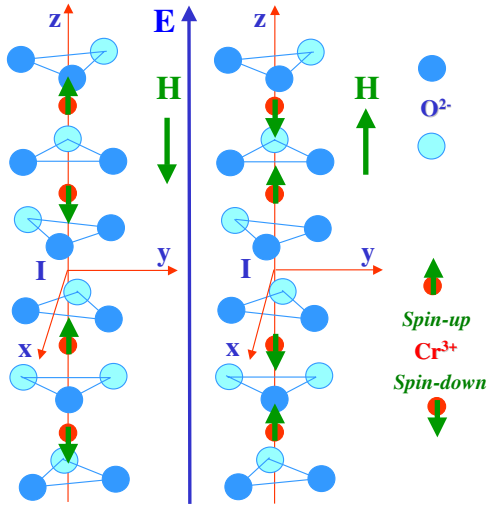

Figure 4. Schematic representation of the two 180° AFM domains grown by ME annealing with (left panel) antiparallel and (right panel) parallel electric ($\boldsymbol{E}$) and magnetic ($\boldsymbol{H}$) fields.

to parity (P) and time reversal (Θ) but is left invariant in the product $P\Theta$. Up to 58 Shubnikov groups are compatible with the ME effect [32]. The generic example of an ME solid is Cr_2O_3: it has a centrosymmetric corundum structure (space group $R\bar{3}c$) but it is reported to have a non-centrosymmetric $\bar{3}'m'$*space-time* group below the Néel temperature $T_N \approx 310$ K. In AFM Cr_2O_3, the easy magnetization direction is along the trigonal $\boldsymbol{c}$-axis. The spin moments can order in either one of the two 180° domains shown in figure 4, which differ because the Cr spin moments have opposite direction with respect to the arrangement of the oxygen ligands. It is easy to check that the two domains shown in figure 4 can be transformed into each other only by a time-reversal operation. It is also obvious that these two domains are uniaxial: one may thus anticipate that by symmetry $\mathrm{Re}\{\zeta^*_{xxz}\} = \mathrm{Re}\{\zeta^*_{yyz}\}$ and consequently no XLMD should be detectable for an x-ray beam propagating along $\boldsymbol{c}$. Nevertheless, a non-reciprocal XMχD signal can still be expected. It should be kept in mind that in equidomain states, no ME effect nor any XMχD can be detected. Fortunately, ME annealing makes it possible to grow single domain states and to switch from one domain to the other: this consists of heating the crystal in its paramagnetic state far above T_N and applying simultaneously along the $\boldsymbol{c}$ axis a modest electric field $\boldsymbol{E}$ (5 kV cm^{-1}) plus a weak magnetic field $\boldsymbol{H}$ ($\pm$0.5 T) before cooling the crystal down well below T_N. Depending on whether $\boldsymbol{E}$ and $\boldsymbol{H}$ are parallel or antiparallel, the free energy of the system is different and a single domain of well characterized sign will grow [33].

The Cr K-edge XMχD spectra displayed in figure 5 were obtained by measuring the XANES spectra at 50 K *after ME annealing* but on subtracting—as a reference—the equidomain XANES spectrum recorded with a crystal heated up to 370 K but cooled down without applying any ($\boldsymbol{E}$, $\boldsymbol{H}$) field. The non-reciprocal nature of the XMχD spectra is thus nicely illustrated by the inverted sign observed when single domains of opposite time reversality are grown by ME annealing. The uniaxial character of the magnetic structure is proved by the fact that we did not observe any significant signal when we tried to record the x-ray linear dichroism (XLD) spectrum reproduced in figure 5 (bottom trace). Moreover, since the rotational isotropy of space is broken when single domains are grown by ME annealing along the direction of ($\boldsymbol{E}$, $\boldsymbol{H}$), one should be able to record XMχD spectra from powdered samples.

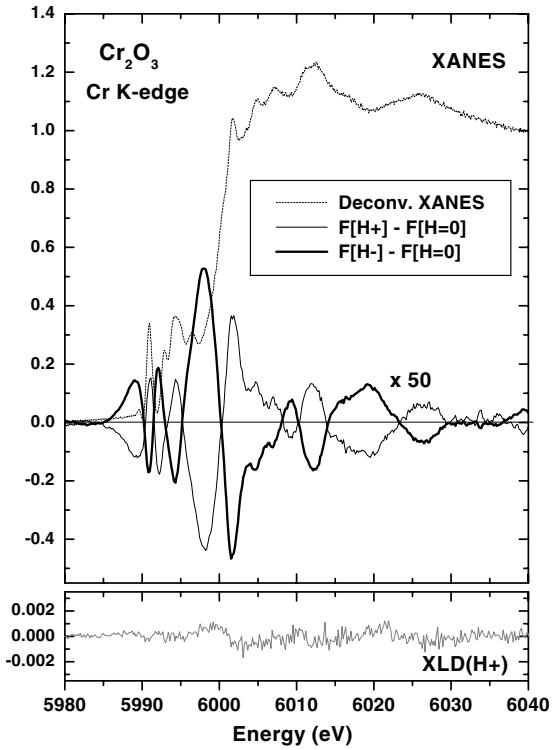

Figure 5. Cr K-edge XMχD spectra of a (001) Cr_2O_3 single crystal for $\boldsymbol{k} \parallel \boldsymbol{c} \parallel \boldsymbol{E} \parallel \boldsymbol{H}$. Equidomain states were taken as reference. The bottom trace reproduces the very weak residual linear dichroism spectrum which was measured and thus confirms the uniaxial character of the structure.

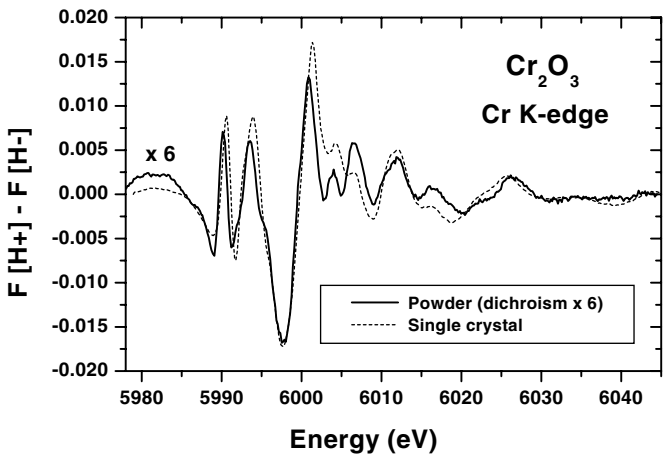

Figure 6. Cr K-edge XMχD spectra of a single crystal Cr_2O_3 or a pellet. Differential absorption refers here to the 180° domains grown by ME annealing.

This is confirmed by figure 6 in which we compare the XMχD spectra recorded either with a pellet of a powdered sample or a single crystal: the two spectra displayed in figure 6 look fairly similar but differ essentially by a 1:6 scaling factor.

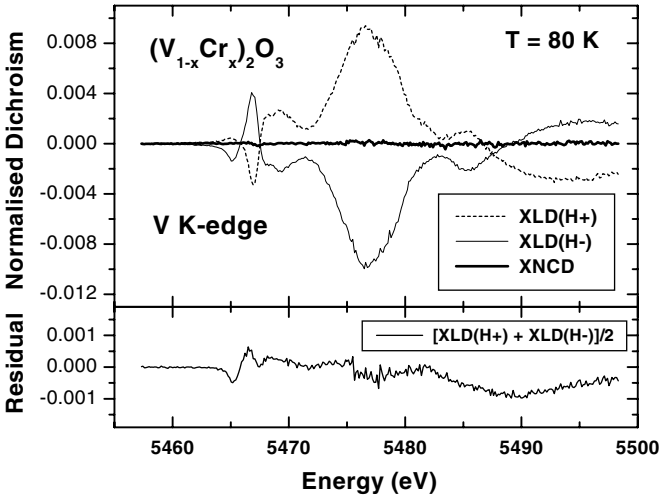

Figure 7. V K-edge *non-reciprocal* XMLD spectra recorded in the monoclinic phase of a $(V_{1-x}Cr_x)_2O_3$ single crystal after ME annealing performed with *parallel* (+) or *antiparallel* (−) electric and magnetic fields. The very weak intensity of the XNCD spectrum displayed at the same scale is fully consistent with a *centrosymmetric* $I2/a$ crystal structure whereas the magnetic structure A2 is *non-centrosymmetric*.

The case of vanadium sesquioxide (V_2O_3) has been known for a long time to be much more puzzling than Cr_2O_3. Recently, there has been renewed interest in V_2O_3 in connection with the questionable orbital ordering model proposed several years ago by Castellani *et al* [34]. We never had any plans to join this important debate but our attention was attracted by a point made by Word *et al* [35] that, according to neutron diffraction data, the space-time group of the AFM monoclinic low temperature phase below T_N should be only **2** due to a transfer of magnetic moments onto oxygen atoms. If this interpretation is correct, then the low-temperature monoclinic phase of V_2O_3 *should* be ME. This consideration prompted us to try to detect any non-reciprocal OA of x-rays in this material. Since the first-order phase transition from the corundum to the monoclinic phase in pure V_2O_3 is known to be crystal destructive, we decided to perform our experiment with a Cr-doped $(V_{1-x}Cr_x)_2O_3$ single crystal for which $x = 0.028$ and $T_N = 181$ K: such a crystal was kindly made available to us by the magnetic diffraction team of the ESRF. According to neutron diffraction data, the magnetic moments (1.2 μ_B/V atom) should be rotated by about 71° with respect to the hexagonal $\boldsymbol{c}$-axis in the monoclinic low-temperature phase: the symmetry condition $\mathrm{Re}\{\zeta^*_{xxz}\} = \mathrm{Re}\{\zeta^*_{yyz}\}$ should then be lost and the system could exhibit non-reciprocal XMLD. As illustrated in figure 7, an experiment [12] performed at the ESRF ID12 beamline seems to support the interpretation proposed by Word and his colleagues since we observed a linear dichroism signal that was inverted when the ME annealing was performed with either parallel or antiparallel electric and magnetic fields ($\boldsymbol{E}, \boldsymbol{H}$). This is the typical behaviour expected for a non-reciprocal time-reversal odd effect. We would also like to point out that in our non-reciprocal XMLD experiment the magnetic field $\boldsymbol{H}$ was collinear with the x-ray wavevector $\boldsymbol{k}$, whereas $\boldsymbol{H}$ has to be perpendicular to the direction of propagation of the incident x-rays in conventional (time-reversal *even*) XMLD experiments [13].

6. Effective operator for orbital parity mixing

Over recent years, edge-selective sum rules have been used with much success to derive from XMCD spectra the ground state (ψ) expectation value of the z component of several magnetic operators: $\langle\psi|\boldsymbol{L}_z|\psi\rangle$, $\langle\psi|\boldsymbol{S}_z|\psi\rangle$ and $\langle\psi|\boldsymbol{T}_z|\psi\rangle$. A similar approach was first proposed by Natoli *et al* [27] for XNCD:

$$\int_{Edge} \frac{\Delta\sigma(\hbar\omega)\,\mathrm{d}(\hbar\omega)}{(\hbar\omega)^2} \propto \langle\psi|\boldsymbol{N}^{(2)}|\psi\rangle$$

but the physical content of the pseudo-deviator $\boldsymbol{N}^{(2)}$ was not transparent. Resorting to powerful spectrum-generating algebras, Carra *et al* [18, 19] have shown recently that all effective operators of OA could be built from only three basic vector operators generating a homogeneous Lorentz subalgebra $so(3, 1)$:

(i) $\boldsymbol{n} = \boldsymbol{r}/r$ is a *polar* vector collinear with the electric dipole moment and which is obviously even with respect to time-reversal symmetry;
(ii) the *orbital* angular momentum $\boldsymbol{L}$ is an *axial* vector with odd time-reversal symmetry;
(iii) the *orbital* anapole operator $\boldsymbol{\Omega} = \mathrm{i}[\boldsymbol{n}, \boldsymbol{L}^2]/2$ is a vector which is odd with respect to *both* parity and time reversal.

The main results obtained by Carra *et al* [19] can be summarized in the following way:

- the ground state expectation value of the z component of the orbital anapole moment $\boldsymbol{\Omega}_z$ is expected to be the key effective operator for XMχD, especially for powdered samples [20];
- the effective operator for XNCD is the time-reversal *even*, rank-2 pseudo-deviator of the product of two time-reversal *odd* vectors: $\boldsymbol{N}^{(2)} = [\boldsymbol{L} \otimes \boldsymbol{\Omega}]^{(2)}$;
- the effective operators for non-reciprocal XMLD look much more complicated since they include the time-reversal *odd*, rank-2 pseudo-deviator: $\boldsymbol{W}^{(2)} = [\boldsymbol{L} \otimes \boldsymbol{n}]^{(2)}$ and a time-reversal odd rank-3 septor $\boldsymbol{\Gamma}^{(3)} = [\boldsymbol{L} \otimes \boldsymbol{L} \otimes \boldsymbol{\Omega}]^{(3)}$.

In our opinion, XMχD offers a fairly unique opportunity to access the $\boldsymbol{\Omega}_z$ component of the *orbital* anapole moment even though it may be difficult in some cases to disentangle $\boldsymbol{\Omega}_z$ from an additional contribution of $\boldsymbol{\Gamma}_z^{(3)}$ [20]. Recall that the concept of an anapole was first introduced in 1958 by Zel'dovich [36] from symmetry considerations but essentially as a useful tool to describe *parity-violating* interactions: for nearly 40 years, atomic physicists were angling for nuclear anapoles [37, 38] until the anapole moment of ^{137}Cs was successfully measured in 1997 [39]. There is a classical picture that was proposed by Zel'dovich himself for the anapole [36]: a toroidal solenoid not only generates an annular magnetic field $\boldsymbol{H}_{a(r)}$ but it also produces an axial current $\boldsymbol{J}_{z(r)}$. Indeed, in solid state physics, annular magnetic fields can result from either spin or orbital currents. That a spin anapole is inherently ME is illustrated in figure 8 and can be easily understood: in the presence of an external *magnetic* field $\boldsymbol{H}$, the energy of each spin carrier (electron) depends on its location on the annular orbit on which the electrons are constrained so that the electron distribution will no longer remain uniform and will induce an *electric* polarization $\boldsymbol{P}$ orthogonal to $\boldsymbol{H}$. This ME polarizability can be implicitly extended to orbital anapoles as well.

Not all ME groups admit the anapole moment as an irreducible representation: it has been established [40, 41] that only 31 ME groups out of 58 satisfy this condition and thus make it possible to detect XMχD spectra [20]. Those groups all have in common the characteristic property that their rank-2 ME tensor should have *antisymmetric* off-diagonal terms. In other words, it can be shown that the total anapole moment, including both the spin and the orbital anapole components, is basically proportional to the *dual* vector of the ME tensor.

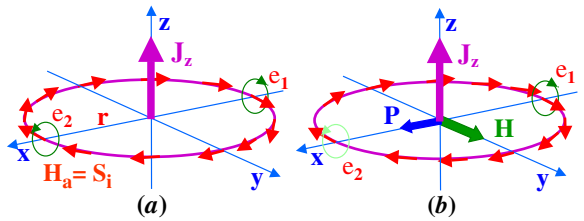

Figure 8. Classical picture of a ME spin anapole. (a) No external magnetic field is applied: the charged spin carrier (electron) distribution is uniform on the annular orbit. (b) With the external magnetic field: the electron distribution is no longer uniform and induces an electric polarization $\boldsymbol{P}$ orthogonal to $\boldsymbol{H}$.

Interestingly, the magnetic group $\bar{3}'m'$ does not admit the anapole as an irreducible representation. This suggests that the true magnetic group of Cr_2O_3 may not be $\bar{3}'m'$ as usually considered on the basis of early neutron data [42] but that it should be lower. There may be several ways to explain such a reduction of the magnetic symmetry. It was our interpretation [11] that the magnetic group could be only $\bar{3}'$. Of course, this would not change anything regarding the chromium spin configuration of the two domains shown in figure 4, but this would imply that there would be some magnetic polarization of the oxygen atoms affecting the *orbital magnetism*. It was pointed out by Samuelsen *et al* [43] 30 years ago that the covalent character in the Cr–O bonds involves a small spin transfer from the chromium 3d orbitals to the oxygen 2p shell, but they noted that this transferred moment is too small to be detected in neutron diffraction experiments. Recall that an asymmetric twist of the oxygen planes is already responsible for a reduction of the local symmetry of the Cr atoms from C_{3v} to C_3 [44]. One may wonder whether the oxygen atoms could not also be responsible for a further lowering of the magnetic symmetry through any speculative polarization transfer mechanism.

7. Conclusion

In this paper we have produced strong evidence that both natural and non-reciprocal OA of x-rays can be measured accurately. We pointed out that in the x-ray regime OA and the gyration tensor are strongly dominated by the E1E2 interference terms whereas the E1M1 terms are well known to dominate at optical wavelengths. We have shown that the x-ray magnetochiral dichroism (XMχD) and the non-reciprocal x-ray magnetic linear dichroism (nr-XMLD) should be very attractive, element-selective new probes of parity non-conserving solids and more specifically of ME solids. In particular, XMχD was shown to give a quite unique access to the local orbital anapole moment at the absorbing site and can be used to unravel hidden space-time symmetry properties in ME solids. In these experiments, the ME effect which we probe requires orbital anapole currents to exist, but not necessarily spin anapole currents. Further work is still in progress in order to extend the field of applications of x-ray OA and to figure out the exact role of the higher-rank effective tensor operators of XNCD and nr-XMLD. This is essential for understanding how orbitals of different parity can be mixed.

Acknowledgments

The authors wish to thank Dr P Carra for providing them with preprints of his recent papers and for many stimulating discussions over the past years. Acknowledgements are also due to Dr E Katz and Dr Y Petroff for their valuable comments and permanent encouragement.

References

[1] Arago D F M 1811 *Mem. Inst. France* (Part 1) **12**
[2] Biot J B 1812 *Mem. Inst. France* (Part 1) **13** 218
[3] Brown W F, Shtrikman S and Treves D 1963 *J. Appl. Phys.* **34** 1233
[4] Birss R R and Shrubsall R G 1967 *Phil. Mag.* **15** 687
[5] Hornreich R M and Shtrikman S 1968 *Phys. Rev.* **171** 1065
[6] Krichevtsov B B, Pavlov V V, Pisarev R V and Gridnev V N 1993 *J. Phys.: Condens. Matter* **5** 8233
[7] Goulon J, Goulon-Ginet C, Rogalev A, Gotte V, Malgrange C, Brouder C and Natoli C R 1998 *J. Chem. Phys.* **108** 6394
[8] Alagna L, Prosperi T, Turchini S, Goulon J, Rogalev A, Goulon-Ginet C, Natoli C R, Peacock R D and Stewart B 1998 *Phys. Rev. Lett.* **80** 4799
[9] Stewart B, Peacock R D, Alagna L, Prosperi T, Turchini S, Goulon J, Rogalev A and Goulon-Ginet C 1999 *J. Am. Chem. Soc.* **121** 10233
[10] Goulon J, Goulon-Ginet C, Rogalev A, Benayoun G, Brouder C and Natoli C R 2000 *J. Synchrotron Radiat.* **6** 673
[11] Goulon J, Rogalev A, Wilhelm F, Goulon-Ginet C, Carra P, Cabaret D and Brouder C 2002 *Phys. Rev. Lett.* **88** 237401–1
[12] Goulon J, Rogalev A, Goulon-Ginet C, Benayoun G, Paolasini L, Brouder C, Malgrange C and Metcalf P 2000 *Phys. Rev. Lett.* **85** 4385
[13] Van der Laan G, Thole B T, Sawatzky G A, Goedkoop J B, Fuggle J C, Esteva J M, Karnatak R, Remeika J P and Dabkowska H A 1986 *Phys. Rev.* B **34** 6529
[14] Buckingham A D 1968 *Adv. Chem. Phys* **12** 107
[15] Barron L D 1982 *Molecular Light Scattering and Optical Activity* (Cambridge: Cambridge University Press)
[16] Graham E B and Raab R E 1992 *Phil. Mag.* **66** 269
[17] Goulon J, Goulon-Ginet C, Rogalev A, Gotte V, Brouder C and Malgrange C 1999 *Eur. Phys. J.* B **12** 373
[18] Carra P, Jerez A and Marri I 2001 *Preprint* cond-mat/0104582
[19] Carra P, Jerez A and Marri I 2002 *Phys. Rev.* B submitted
[20] Goulon J, Rogalev A, Wilhelm F, Goulon-Ginet C, Carra P, Jerez A, Marri I and Brouder C 2002 *J. Exp. Theor. Phys.* submitted
[21] Goulon J, Rogalev A, Gauthier C, Goulon-Ginet C, Pasté S, Signorato R, Neuman C, Varga L and Malgrange C 1998 *J. Synchrotron Radiat.* **5** 232
[22] Rogalev A, Goulon J, Goulon-Ginet C and Malgrange C 2001 *Magnetism and Synchrotron Radiation (Springer Lecture Notes in Physics vol 565)* ed E Beaurepaire *et al* (Berlin: Springer) p 60
[23] Rogalev A, Goulon J, Benayoun G, Elleaume P, Chavanne J, Penel C and Van Vaerenbergh P 1999 *Proc. SPIE* **3773** 275
[24] Goulon J, Goulon-Ginet C, Rogalev A, Benayoun G, Malgrange C and Brouder C 1999 *Proc. SPIE* **3773** 316
[25] Malgrange C, Varga L, Gilès C, Rogalev A and Goulon J 1999 *Proc. SPIE* **3773** 326
[26] Jerphagnon J and Chemla D 1976 *J. Chem. Phys.* **65** 1522
[27] Natoli C R, Brouder C, Sainctavit Ph, Goulon J, Goulon-Ginet C and Rogalev A 1998 *Eur. Phys. J.* B **4** 1
[28] Ankudinov A L and Rehr J J 2000 *Phys. Rev.* B **62** 2437
[29] Benayoun G 2001 *PhD Thesis* Université J Fourier, Grenoble
[30] Joly Y 2001 *Phys. Rev.* B **63** 125120
[31] Dzyaloshinskii I 1991 *Phys. Lett.* A **155** 62
[32] Rivera J P 1994 *Ferroelectrics* **161** 165
[33] Brown P J, Forsyth J B and Tasset F 1998 *J. Phys.: Condens. Matter* **10** 663
[34] Castellani C, Natoli C R and Ranninger J 1978 *Phys. Rev.* B **18** 4945
[35] Word R E, Werner S A, Yelon W B, Honig J M and Shivashankar S 1981 *Phys. Rev.* B **23** 3533
[36] Zel'dovich Ia B 1958 *Sov. Phys.–JETP* **6** 1184
[37] Khriplovich I B 1991 *Parity Non-Conservation in Atomic Phenomena* (New York: Gordon and Breach)
[38] Bouchiat M A and Bouchiat C 1997 *Rep. Prog. Phys.* **60** 1351
[39] Wood C S, Bennett S C, Cho D, Masterson B P, Roberts J L, Tanner C E and Wieman C E 1997 *Science* **275** 1759
[40] Asher E 1974 *Phys. Status Solidi* b **65** 677
[41] Dubovik V M, Krotov S S and Tugushev V V 1988 *Sov. Phys.–Crystallogr.* **32** 314
[42] Brockhouse B N 1953 *J. Chem. Phys.* **21** 961
[43] Samuelsen E J, Hutchings M T and Shirane G 1970 *Physica* **48** 13
[44] Vallade M 1968 *PhD Thesis* Université J Fourier, Grenoble